

# Effect of Chemical and Mechanical Actions on the Micro-morphology evolution in CMP

Ping Zhou<sup>#</sup>, Tao Wu and Hongyu Di

State Key Laboratory of High-performance Precision Manufacturing, Dalian University of Technology, Dalian 116024, China  
<sup>#</sup> Corresponding Author / Email: pzhou@dlut.edu.cn, TEL: +86-134-7875-4767

KEYWORDS: Chemical mechanical polishing, Atomic-level roughness, Surface micro-morphology, Chemical-mechanical synergy

---

*How to obtain atomically smooth surfaces is one of the focus issues in precision machining field, and chemical mechanical polishing (CMP) is the most popular method for obtaining ultra-smooth and untrla-falt surfaces. This work focuses on revealing the influencing factors of the surface roughness of polished workpieces. During the CMP process, the evolution of surface micro-topography is collectively influenced by various polishing parameters. Clarifying the relationship between these factors is a very difficult but also very interesting work. This work studies the influence of various factors on the evolution of the power spectral density (PSD) of the micro-morphology of the workpiece surface, from the perspective of the chemical reaction rate and the mechanical removal rate, through typical material polishing experiments and theoretical model analysis. The research results show that the polishing slurry and process parameters can be explained in terms of the activation rate of surface atoms and the removal rate of activated atoms under the mechanical action of abrasive particles. This research has guiding significance for the development of atomic-level surface polishing processes.*

---

## 1. Introduction

Chemical Mechanical Polishing (CMP) is a critical technology for fabricating ultra-smooth surfaces with near-atomic roughness, widely used in the manufacturing of integrated circuits and optical components [1]. The micro-scale surface topography is the most concerned in CMP process, and also plays a vital role in determining the performance of devices. Due to the complex interplay of chemical and mechanical interactions in CMP, process optimization often relies on iterative trial-and-error guided by empirical knowledge [2]. Thus, a comprehensive understanding of surface topography evolution during CMP is essential to achieve optimal polishing outcomes.

In CMP, the chemical effect involves the formation of a reaction layer on the workpiece surface through chemical reactions between the slurry components and the substrate material. This reaction layer make it more susceptible to abrasion by the mechanical action of the polishing process [3][4]. Simultaneously, the mechanical effect in CMP is governed by the physical abrasion by abrasive particles and the properties of the polishing pad [5], as well as the polishing pressure. These abrasive particles remove the reaction layer and a certain amount of the underlying material [6]. The efficiency of material removal and the resulting surface roughness depend on a delicate balance among abrasive particle size, distribution, applied pressure, and pad characteristics [7]. Higher mechanical forces or larger abrasive particles

can increase the material removal rate but may also lead to defects such as scratches, while insufficient forces may result in low removal rates and poor surface quality. Therefore, optimizing the CMP process requires a precise balance between chemical and mechanical effects to achieve minimal surface roughness while avoiding surface defects.

In this study, experimental data from typical polishing tests were integrated with theoretical modeling to investigate the evolution of surface morphology during the CMP process. The focus was placed on how the chemical properties of the slurry and various process parameters collectively influence the surface morphology, taking into account the chemical reaction rates and the mechanical material removal rates.

## 2. Experimental method

The experimental workpieces used in this study were commercially available single-crystal silicon (100) wafers, provided by Lijing Electronics Co., Ltd. It has an elastic modulus of 130 GPa, and a Poisson's ratio of 0.28. The polishing slurry employed was a commercially available silica sol from FUJIMI Corporation. The initial abrasive concentration in the slurry was 40% by mass. The slurry was then diluted to a 10% abrasive concentration, and its pH was stabilized using a KOH solution. For the polishing process, a Politex polishing pad was utilized. Its Young's modulus is 80Mpa.

Prior to the main experiments, the single-crystal silicon workpieces were ground with 1200-grit sandpaper to remove the oxide and defect layers from the surface of both samples and achieve a uniform surface roughness of approximately Sa 22 nm. The original silica sol slurry was mixed with deionized water and stirred for 20 minutes before being continuously supplied to the workpiece surface during the experiment, with constant stirring throughout. The CMP experiments were conducted using a fully automated polisher. The single-crystal silicon samples were secured to the polishing head using stainless steel molds. The polishing pad rotated at 70 rpm, while the workpieces rotated at 65 rpm, with a slurry flow rate of 15 ml/min. The polishing was stopped every 10 minutes to measure the surface topography.

Due to the varying spatial frequency bandwidth limitations of different measurement instruments, it is necessary to use devices with different resolutions to capture data across multiple frequency ranges. A 3D optical surface profiler (ZYGO) (NewView9000, ZYGO Corporation, USA) and an Atomic Force Microscope (AFM) (NTEGRA II, NT-MDT Spectrum Instruments, Russia) were employed for surface measurements. The ZYGO profiler has a lateral resolution of 340 nm and a vertical resolution of 0.08 nm, with a scanning area of  $868.148 \mu\text{m} \times 868.148 \mu\text{m}$ . The measured surface was processed using Gaussian filtering, with a sampling length of 80  $\mu\text{m}$ . The AFM, on the other hand, provides a higher lateral resolution of 1 nm and a vertical resolution of 0.01 nm, with a scanning area of  $10 \mu\text{m} \times 10 \mu\text{m}$ , covering  $256 \times 256$  pixels with a point spacing of 0.039  $\mu\text{m}$ .

### 3. Results and discussion

#### 3.1 The influence of mechanical action

Single-crystal silicon, pre-ground with sandpaper, was polished for 1 hour under polishing pressures of 0.12 MPa and 0.04 MPa. The slurry's pH was set to 10. Before CMP, the initial surface roughness of the workpiece was Sa 23 nm measured by ZYGO and Sa 22 nm measured by AFM. Fig. 1 shows the surface micro-topography images obtained after 5 minutes, 20 minutes, and 40 minutes of polishing, respectively. The results indicate that as CMP progresses, the surface profile of the workpiece becomes increasingly uniform, and minor scratches and corrosion pits are gradually eliminated. Notably, under higher polishing pressures, both mid-frequency and high-frequency errors converge faster and reach higher ultimate convergence values.

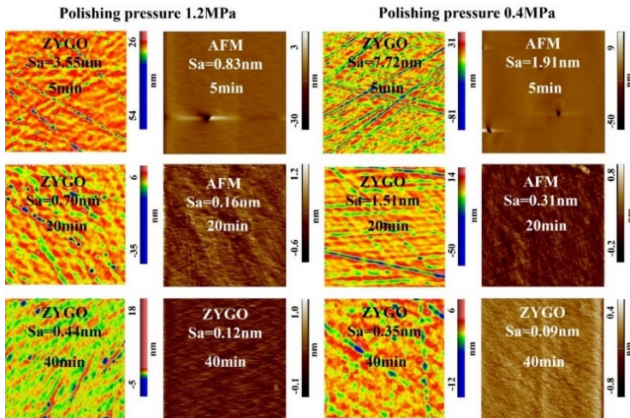


Fig. 1. Evolution results of roughness Sa under different polishing pressures

The time it takes for the surface micro-topography to reach a stable state during CMP, known as the convergence time, can be directly observed through the evolution of surface roughness Sa. Fig. 2 illustrates the surface roughness Sa evolution under different abrasive particle sizes. It is evident that under a polishing pressure of 0.12 MPa, the surface roughness converged to its minimum value at 30 minutes, while under 0.04 MPa, it took 40 minutes to reach convergence. At steady-state, the surface roughness stabilized at 0.43 nm and 0.33 nm on the ZYGO, and at 0.12 nm and 0.09 nm on the AFM for polishing pressures of 0.12 MPa and 0.04 MPa, respectively.

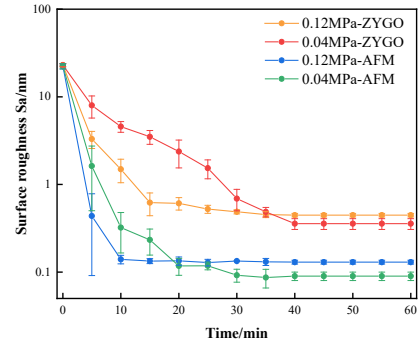


Fig. 2. Evolution of surface roughness Sa under different polishing pressures

#### 3.2 The influence of chemical reactions

In this section, the chemical effects during the CMP process were adjusted by varying the pH of the polishing slurry. Single-crystal silicon, pre-ground with sandpaper, was polished for 1 hour using slurries with pH values of 10 and 12. Table 2 presents the evolution of surface roughness Sa under different pH conditions. It shows that with a slurry of pH = 12, the roughness reached its minimum value after 30 minutes, while for a slurry of pH = 10, it took 40 minutes to converge. At steady state, the surface roughness stabilized at 0.34 nm and 0.49 nm on the ZYGO, and at 0.10 nm and 0.21 nm on the AFM for pH = 10 and pH = 12, respectively.

Table 2. Evolution of surface roughness Sa under different pH slurries

PH	Time/min	Sa/nm (ZYGO)	Sa/nm (AFM)
10	10	2.71	1.08
10	20	0.87	0.22
10	30	0.48	0.13
10	40	0.35	0.10
10	60	0.34	0.10
12	10	1.28	0.61
12	20	0.51	0.24
12	30	0.49	0.22
12	40	0.50	0.21
12	60	0.49	0.21

When using a pH = 12 slurry, the convergence rate of mid- and high-frequency errors was faster than with a pH = 10 slurry. Moreover, the ultimate mid- and high-frequency errors were larger for pH = 12 compared to pH = 10.

At the spatial scale measured by AFM, the curvature radius of local low points on the workpiece surface is generally smaller than the radius of the abrasive particles. This results in a higher probability of

abrasives contacting and effectively removing the high points on the surface profile, while the likelihood of contact with low points is reduced, leading to less effective removal. When the pH of the slurry is increased to 12, the formation rate of the reaction layer on the workpiece surface accelerates, resulting in a deeper reaction layer over the same time period. This enhances the removal capability of the abrasives for high points on the surface profile, while the removal rate for low points remains largely unchanged compared to pH = 10.

On the spatial scale measured by ZYGO, the actual contact area between the polishing pad and the workpiece surface is relatively small. The polishing pad primarily contacts the high points on the surface profile, with only a few rough peaks of the pad reaching the low points. As a result, the removal rate of the high points is faster. When the slurry pH is increased, the reaction layer forms more rapidly, leading to more effective removal of high points by the polishing pad. However, only a few rough peaks can still contact the low points, thereby enhancing the ability to reduce the height difference between high and low points on the surface profile. Consequently, the convergence rate of mid-frequency errors is faster for a pH = 12 slurry than for a pH = 10 slurry.

### 3.3 Numerical simulation

A numerical simulation model has been developed in our previous work to account for the synergistic effects of chemical and mechanical actions on the evolution of surface micro-topography [8]. This model reveals the influence mechanisms of both chemical and mechanical actions on surface micro-topography and can be used to guide the optimization of CMP process parameters in engineering applications.

In the CMP process, hydroxides present in the polishing slurry oxidize silicon atoms on the workpiece surface, forming a reaction layer with mechanical properties different from those of the substrate. The depth of this reaction layer, along with the material removal depth by abrasive particles, directly influences the material removal rate (MRR) in CMP.

#### 3.3.1 Analysis of Chemical Reaction Parameters

The chemical effect coefficient  $K_c$  primarily reflects the evolution rate of the reaction layer depth on the workpiece surface. Factors such as slurry pH, oxidizer concentration, and workpiece material influence  $K_c$ . By calibrating  $K_c$ , the evolution pattern of the reaction layer depth under specific conditions can be determined. To explore how the chemical effect parameter  $K_c$  affects the evolution of surface micro-topography during CMP, numerical simulations were performed using  $K_c$  values of  $1 \times 10^4 \text{ L} \cdot \text{mol}^{-1} \cdot \text{s}^{-1}$ ,  $2 \times 10^4 \text{ L} \cdot \text{mol}^{-1} \cdot \text{s}^{-1}$ ,  $3 \times 10^4 \text{ L} \cdot \text{mol}^{-1} \cdot \text{s}^{-1}$ ,  $4 \times 10^4 \text{ L} \cdot \text{mol}^{-1} \cdot \text{s}^{-1}$  and  $5 \times 10^4 \text{ L} \cdot \text{mol}^{-1} \cdot \text{s}^{-1}$ . The initial surface roughness input for the numerical simulations was set at Ra 10 nm. The time for the surface micro-topography to evolve to its minimum value under different  $K_c$  values is shown in Fig. 3 (a). It can be observed that as the  $K_c$  value increases, the convergence rate of the surface micro-topography accelerates, showing a nonlinear relationship. When  $K_c$  is small, the reaction layer depth on the workpiece surface evolves slowly, and the abrasives can completely remove the reaction layer during CMP. In this case, the evolution rate of the surface micro-topography is limited by the reaction layer depth, resulting in slower convergence.

Conversely, when  $K_c$  is large, the reaction layer depth evolves more rapidly, and the removal depth of the abrasives is less than the reaction layer depth. In this scenario, the surface micro-topography evolution is not restricted by the reaction layer, leading to faster convergence.

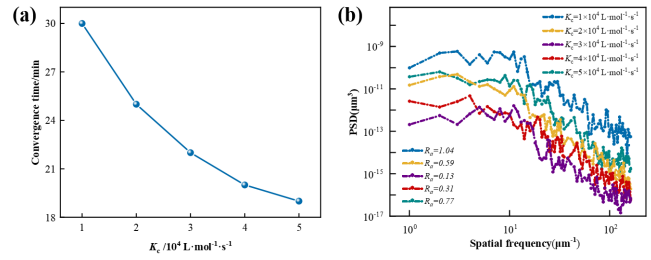


Fig. 3 . Simulation results with different chemical action. (a) Convergence time of surface microtopography. (b) The stability value of surface microtopography.

The final limit values of surface micro-topography evolution under different  $K_c$  values are illustrated in Fig. 3 (b). As the  $K_c$  value increases, the final limit of surface micro-topography first decreases and then increases. When  $K_c$  is low, the chemical reaction capacity is weaker than the mechanical removal capacity, and the material removal process is dominated by chemical reactions, resulting in a relatively poor surface micro-topography. As the  $K_c$  value gradually increases, the mechanical removal capacity and chemical reaction capacity become more balanced. When both are equal, the surface microtopography reaches an optimal state, with the corresponding surface roughness value achieving as low as 0.13 nm. However, if the  $K_c$  value continues to increase, the mechanical removal capacity becomes weaker than the chemical reaction capacity, causing the material removal process to be dominated by chemical action, again leading to a poorer surface micro-topography. These numerical simulation results align with experimental findings, further confirming that the evolution of surface micro-topography is determined by the combined effects of chemical and mechanical actions.

#### 3.3.2 Analysis of Mechanical Parameters

The mechanical effect parameter  $K_m$  primarily reflects the removal depth of abrasives on the workpiece surface during CMP. Factors such as polishing pressure, polishing speed, abrasive particle size, and the mechanical properties of the polishing pad affect  $K_m$ . By calibrating  $K_m$ , the removal depth of the workpiece surface under specific conditions can be determined. In the CMP process, there may be three scenarios regarding material removal by abrasives: the abrasives cannot completely remove the reaction layer; the abrasives can remove the reaction layer but not the substrate material; the abrasives can remove both the reaction layer and the substrate material. To explore the evolution of surface micro-topography under these three different scenarios, numerical simulations were conducted using  $K_m$  values of 0.1, 0.5, 1.0, 1.5, and 2.0. The initial surface roughness for the simulations was set to Ra 10 nm.

The time required for the surface micro-topography to reach its minimum value under different  $K_m$  values is shown in Fig. 4 (a). Initially, as  $K_m$  increases, the convergence rate of surface micro-topography accelerates. After this phase, the convergence rate slows down, and a stable stage appears as  $K_m$  continues to increase. In the

final phase, the convergence rate decreases further with increasing  $K_m$ . When  $K_m$  is small, the mechanical removal effect of the abrasives is weak, leading to a low material removal rate and slow convergence of surface micro-topography. As  $K_m$  increases, the material removal rate accelerates, and the convergence rate of surface micro-topography increases. However, once  $K_m$  reaches a certain level, the convergence rate slows down due to the limitation imposed by the reaction layer. The convergence rate accelerates again when  $K_m$  becomes large enough to remove the substrate material.

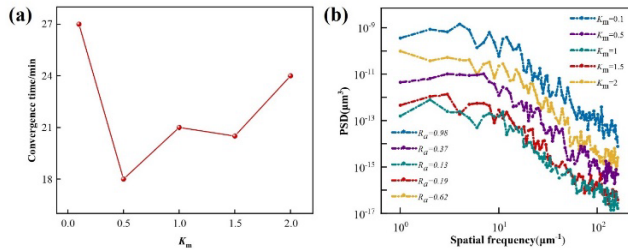


Fig. 4. Simulation results with different mechanical action. (a) Convergence time of surface microtopography. (b) The stability value of surface microtopography.

The final limit values of surface micro-topography evolution under different  $K_m$  values are shown in Fig. 4 (b). As  $K_m$  increases, the final evolved limit of the surface micro-topography first decreases and then increases. During CMP, when  $K_m$  is small, the chemical reaction capacity is stronger than the mechanical removal capacity, resulting in a material removal process dominated by chemical action and, consequently, a poor surface micro-topography. As  $K_m$  gradually increases, the mechanical removal capacity approaches the chemical reaction capacity, leading to an improved surface micro-topography. However, as the value of  $K_m$  continues to increase, the mechanical removal capability surpasses the chemical reactivity, resulting in a material removal process dominated by mechanical action. This shift leads to a deterioration in surface microtopography, with surface roughness worsening from 0.13 nm to 0.62 nm. At this point,  $K_m$  is not sufficient to remove the substrate material, and the removal depth of abrasives is limited by the reaction layer. When  $K_m$  is at a stage where it can fully remove the reaction layer but not the substrate material, the final limit values of surface micro-topography are similar. As  $K_m$  continues to increase and the force applied to the abrasives reaches the yield limit of the substrate material, the removal depth of the abrasives is no longer constrained by the reaction layer. In this stage, the removal depth increases with  $K_m$ , the removal rate accelerates, and the surface micro-topography deteriorates.

## Conclusion

The evolution of surface micro-topography during Chemical Mechanical Polishing (CMP) was investigated from two critical perspectives: mechanical and chemical effects. By varying polishing pressure, and slurry pH, the mechanical and chemical interactions within the CMP process were systematically adjusted. The resulting surface topography evolution was analyzed using the changes in power spectral density (PSD) curves. Additionally, a numerical simulation model was developed to account for the synergistic effects of chemical and mechanical actions on the evolution of surface micro-topography.

This model incorporates the dynamic evolution of the depth of the chemical reaction layer on the workpiece surface and the material removal efficiency of abrasives, providing a deeper understanding of the mechanisms governing surface topography changes during CMP. The findings indicate that both strong chemical and mechanical effects significantly accelerate the evolution of surface micro-topography. The pH value of the slurry significantly affects the chemical reaction rate between the workpiece surface and the slurry components. Different polishing process parameters correspond to varying intensities of mechanical action. Higher polishing pressure accelerates the convergence rate across all spatial frequencies. Therefore, achieving a balance between chemical and mechanical effects is crucial in practical polishing processes.

## ACKNOWLEDGEMENT

The authors acknowledge the financial support from the National Natural Science Foundation of China (Grant No.52375409, No. 51991373).

## REFERENCES

1. Khanna, A., J. Kakireddy, V. R., Fung, J. and et al., "Engineering Surface Texture of Pads for Improving CMP Performance of Sub-10 nm Nodes," ECS J. Solid State Sci. Technol., Vol. 9, pp. 104003, 2020.
2. Tao, H., Zeng, Q., Liu, Y. and et al., "Effects of grinding-induced surface topography on the material removal mechanism of silicon chemical mechanical polishing," Appl. Surf. Sci., Vol. 631, pp. 157509, 2023.
3. Chen, L., He, H., Wang, X. and et al., "Tribology of Si/SiO<sub>2</sub> in Humid Air: Transition from Severe Chemical Wear to Wearless Behavior at Nanoscale," Langmuir, Vol. 31, pp. 149-156, 2015.
4. Filatov, Y.D., "Polishing of Precision Surfaces of Optoelectronic Device Elements Made of Glass, Sital, and Optical and Semiconductor Crystals: A Review," J. Superhard Mater., Vol. 42, pp. 30-48, 2020.
5. Guo, X., Yuan, S., Huang, J. and et al., "Effects of pressure and slurry on removal mechanism during the chemical mechanical polishing of quartz glass using ReaxFF MD," Appl. Surf. Sci., Vol. 505, pp. 144610, 2020.
6. He, H., Hahn, S. H., Yu, J. and et al., "Friction-induced subsurface densification of glass at contact stress far below indentation damage threshold," Acta Mater., Vol. 189, pp. 166-173, 2020.
7. Jiang, B., Zhao, D., Wang, B. and et al., "Flatness maintenance and roughness reduction of silicon mirror in chemical mechanical polishing process," Sci. China Technol. Sci., Vol. 63, pp. 166-172, 2020.
8. Yang, K., Huang, N., and Di, H. and et al., "Modeling of surface microtopography evolution in chemical mechanical polishing considering chemical-mechanical synergy," Tribol. Int., Vol. 201, pp. 110206, 2025.